Crystallization and shape emulation in atactic poly(vinyl chloride) and polyacrylonitrile*

R. J. Hobson‡ and A. H. Windle†
Department of Materials Science and Metallurgy, University of Cambridge, Pembroke Street, Cambridge CB2 3QZ, UK
(Received 11 September 1992; revised 24 February 1993)

Molecular modelling calculations have been used to explore the unexpectedly large values of crystallinity measured in atactic poly(vinyl chloride) (PVC) and polyacrylonitrile (PAN). Using MOPAC V:AM1 (distributed by QCPE), it was found that not only can a chain of isotactic PVC (and PAN) emulate the shape and axial repeat of an equivalent (planar zigzag) syndiotactic molecule, but that the shape-emulating conformation has its own energy minimum. This conformation is similar to that first suggested by Juijn. It appears that the dipole interactions between adjacent hydrogen and chlorine atoms are able to stabilize this conformation even though there is no minimum apparent on a two-dimensional energy map corresponding to one repeat unit. Calculations on longer sequences show that this conformation has a subsidiary energy minimum. Similar behaviour has been found in the case of PAN. Wide-angle X-ray diffraction from PVC crystals composed of syndiotactic and isotactic monomer units (but using established unit cell dimensions) was simulated using CERIUS (Molecular Simulations Ltd, Cambridge, UK). The crystalline component of the experimental diffraction profile was found to correspond to that calculated for a mixed tacticity lattice. Furthermore, the relative intensities of the 200 and 110 diffraction maxima have been shown to give a good indication of the mean chain tacticity within the crystallites which can be related to the overall tacticity of the polymer. Calculations of crystallinity content based on mixed tacticity lattices (where dyad tacticity = 0.55) were found to be consistent with the crystallinity and crystallite thickness observed experimentally (10% and 33 Å), whereas these observations are quite inexplicable if the only crystallizable sequences are syndiotactic. A similar predicted relationship between lattice tacticity and relative intensity of the 200 and 110 peaks could not be confirmed for PAN as the almost pseudo hexagonal chain packing means that the 200 and 110 peaks are all but superimposed in the experimental plots. It is noted that extra low angle reflections are found in the simulations of mixed tacticity crystallites where the models are not large enough to ensure a completely random distribution of the isotactic, shape-emulating sequences, if they have been arranged with any degree of periodicity. Low angle reflections have also been observed experimentally. Hence, although PAN does not have the 200/110 WAXS fingerprint of PVC, there is, in addition to the general observation of high crystallinity for the atactic polymers, experimental evidence for co-crystallization of the configurational isomers.

(Keywords: PVC; PAN; WAXS; molecular modelling; crystallinity; MOPAC; CERIUS)

INTRODUCTION

The basis for the existence of crystallinity in atactic polymers was first discussed by Flory in 1955[1]. He proposed that atactic chains are not necessarily prevented from taking part in crystallization just because they are random, but may form crystallites by virtue of the mutual segregation of crystallizable sequences. A development of this model, in the 1980s, arose from studies of crystallization in random copolyesters[2–4]. In these materials, similar but aperiodic sequences segregate to form thin crystallites that are based on non-periodic layers.

An ongoing issue in the area of polymer crystallization concerns the level of crystallinity which is observed in commercial poly(vinyl chloride) (PVC) despite the polymer being almost completely atactic (syndiotactic dyads 55%). Furthermore, surprisingly high levels of crystallinity are observed also in atactic polyacrylonitrile (PAN) (syndiotactic dyads $\approx$ 40%). Although a wealth of experimental work devoted to the characterization of order in PVC and PAN has been published over recent years, several key issues remain unresolved, the most notable being the question as to how comparatively high levels of order can be observed in these two almost atactic polymers and yet not in other vinyl-type polymers such as nominally atactic poly(methyl methacrylate) (syndiotactic dyads 80%) and polystyrene[5]. This paper re-examines the experimental evidence for crystallization in PVC and PAN and specifically addresses the outstanding issues by applying modern methods of molecular modelling.

* Presented at 'Polymer Science and Technology' – a conference to mark the 65th birthday of Professor Ian Ward FRS, 21–23 April 1993, University of Leeds, UK

† To whom correspondence should be addressed
‡ Present address: Minnesota 3M Research Ltd., Harlow, Essex CM19 5AE

0032-3861/93/173582-15

POLY(VINYL CHLORIDE)

Previous studies on PVC structure

PVC is well known as a semicrystalline monosubstituted vinyl polymer composed of randomly disposed syndiotactic and isotactic units. Generally speaking, samples produced commercially contain a slightly greater proportion of syndiotactic dyads than isotactic dyads, n.m.r. measurements[6] giving the dyad tacticity to be ~55% (or 0.55). The crystallinity in a commercial PVC resin is of the order of 10%, although the actual level depends on the exact polymerization conditions used. Both the temperature and polymerization method affect the tacticity and the crystallinity is seen to rise as the polymer becomes more syndiotactic (*Figure 1*)[7-10]. Natta and Corradini attributed the observed crystallization solely to segregated syndiotactic sequences[11], however Kockott[12] has pointed out subsequently that the concentration of such sequences is insufficient to account for both the observed crystal thickness and crystallinity.

The earliest crystal structure, assigned by Natta and Corradini[11], was deduced from the wide-angle X-ray scattering (WAXS) from a predominantly atactic fibre. The diffracting crystallites were found to be composed of syndiotactic chains in planar zigzag conformation arranged on an orthorhombic lattice. This structure was later supported by Wilkes *et al.*[13] who examined highly syndiotactic PVC prepared using a polymerization method developed by Burleigh[14] and crystallized from a 0.1% solution in chlorobenzene. The structure determined by Wilkes *et al.* is shown in *Figure 2* as a *c* axis projection. The dimensions of the unit cells from these two studies and a third deduced by Nakajima and Hayashi[15] are compared in *Table 1*. The literature tends to imply that, since the crystallinity in the more highly syndiotactic material is greater, and the experimental difficulties thus reduced, the data of Wilkes *et al.*, in particular, represent a refinement of the original Natta and Corradini measurements. However, the possibility of there being a real relationship between tacticity and lattice parameters, is not to be discarded and, in fact, features prominently in the understanding developed below.

The resin used by Natta and Corradini was of low tacticity with both density[16] and X-ray diffraction

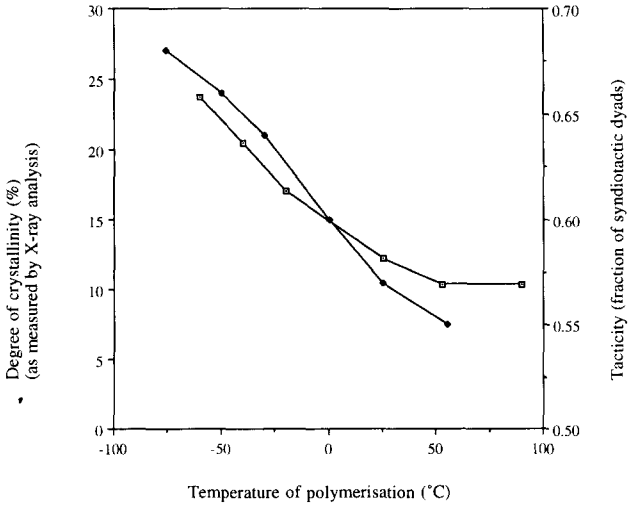

Figure 1 Dependence of (□) crystallinity and (◆) tacticity on the temperature of free radical polymerization of PVC. Data obtained from references 7–10

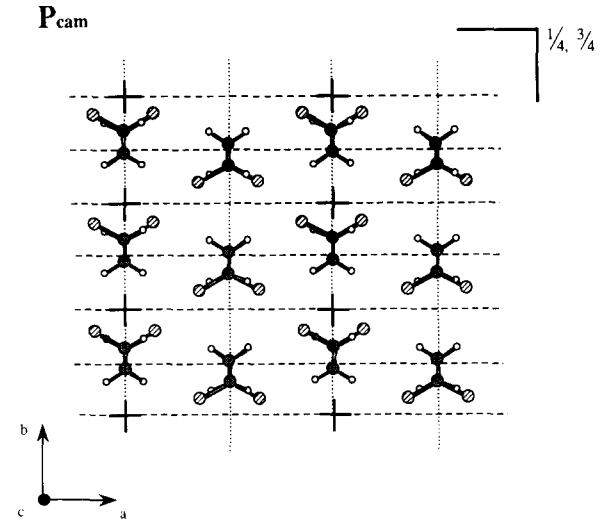

Figure 2 Orthorhombic structure of syndiotactic PVC[13] (*c* axis projection)

Table 1 Orthorhombic unit cell dimensions for crystalline PVC

Sample	*a* (Å)	*b* (Å)	*c* (Å)
Commercial PVC (polymerized at 50–60°C)[11]	10.6	5.40	5.10
Single crystals (polymerized at −75°C)[15]	10.32	5.32	–
Single crystals (made in n-butyraldehyde)[13]	10.24	5.24	5.08

measurements[8-10] suggesting a crystallinity of between 10% and 11%. However, it is also known[12,17,18] that there is an insufficient number of syndiotactic sequences of adequate length to account for both 10% crystallinity and the measured crystal thickness in the chain direction. Lemstra *et al.*[19] determined the average crystallite thickness (commercial PVC, crystallinity 10%) to correspond to 13 monomer units, which is almost twice the length that would be compatible with the measurements of tacticity and crystallinity. Put another way, this means that if all syndiotactic sequences of 13 monomer units or more were to segregate and crystallize then the maximum crystallinity possible would be 0.27%[17,18,20]. This central dichotomy was recognized and investigated by Juijn in 1972[17,18] who suggested that some isotactic monomer units must be included in the otherwise syndiotactic PVC crystallites in order to account for an observed crystallinity of 10%. The implication is that the conformation of any isotactic sequences must be such that their shape and axial repeat is sufficiently similar to that of the syndiotactic planar zigzag chains to enable them to be incorporated in the crystal. (We refer to this special conformation as 'shape-emulating'.) It appears that the general shape of isotactic sequences will emulate that of a syndiotactic planar zigzag chain if every alternate backbone torsion angle is rotated, one way and then the other, by ~30° away from the planar zigzag setting. *Figure 3* compares pictorially, the shape and axial repeat of a syndiotactic planar zigzag molecule with an isotactic molecule in the shape-emulating conformation. When it was published, Juijn's proposal presented an elegant solution to the problem of the observed crystallinity in atactic PVC. To

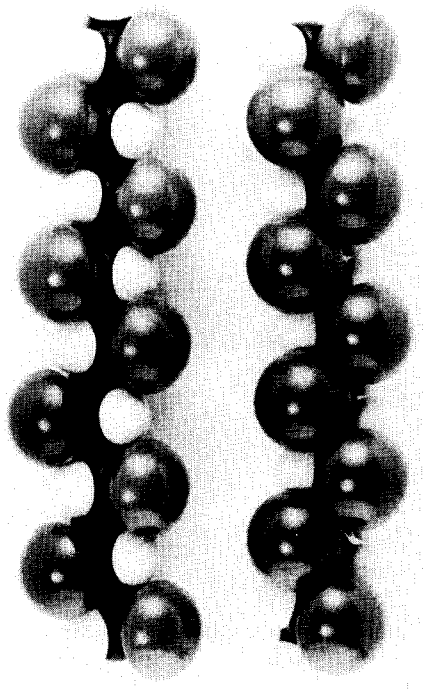

Figure 3 CPK models representing: (left) syndiotactic planar zigzag PVC; (right) isotactic PVC in a conformation which emulates the shape of the planar zigzag syndiotactic PVC

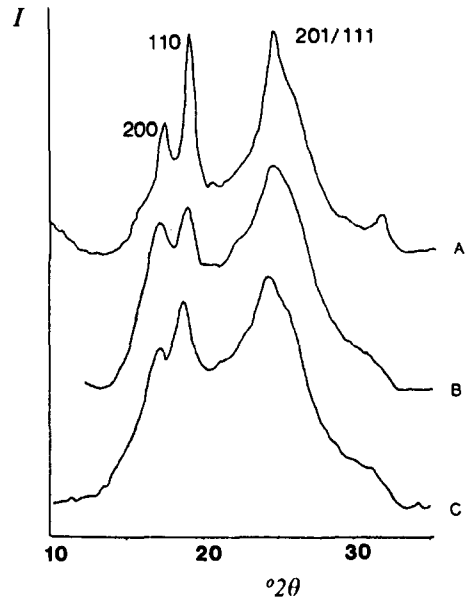

Figure 4 X-ray powder diffraction scans of PVC (reproduced from reference 26): (A) high crystallinity PVC (polymerized in the presence of n-butyraldehyde); (B) commercial PVC (PP 220. Petroplas); (C) plasticized commercial PVC

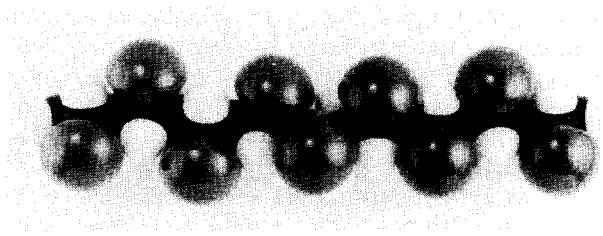

Figure 5 A CPK model of PVC showing how two consecutive isotactic monomer units, in the shape-emulating conformation, can be accommodated into a syndiotactic PVC chain without any appreciable change in shape. (Note, the defect starts on the fourth chlorine atom from the left)

date, however, no conclusive experimental evidence has been found to support the model which is also difficult to define from the original paper. Indeed, Keller[21], in a review, suggested that the unusually high crystallinity value could be due, equally, to syndiotactic sequences grouping together in a more blocky manner than is suggested by the simple statistical treatment of the n.m.r. data.

Keller also discovered two different populations of PVC crystallites[22,23]. Prior to this finding, PVC was understood to crystallize in a fringed micelle manner with the crystallites acting as junction points tying together the amorphous phase to give a thermoreversible crosslinked gel (it is this intrinsic network that allows PVC to be so usefully plasticized unlike most other amorphous polymers). A second, lamellar form of crystallization was found when the polymer was gelled from solution[22,23]. The two different crystallite populations (having the same orthorhombic crystal structure[24]), were distinguished by their different orientations in the drawn polymer; the fringed micelle type showing the usual *c* axis alignment with the drawing direction, while the second type was seen to align with the *a* axis parallel to the draw direction.

Mammi and Nardi[25] noted another structural abnormality when they observed the appearance of a 'curious ring' at $2\theta = 5.4°$ in the fibre diffraction of PVC samples, which had been stretched and then allowed to shrink. In addition, it is apparent from several more recent papers[26–28], that the WAXS powder diffraction pattern of commercial atactic PVC is not simply a broadened version of the highly syndiotactic PVC pattern, and that changes to the powder diffraction have been observed as a consequence of either mechanical treatment or different methods of polymerization of the sample. As one example, the WAXS profiles recorded by Guerrero *et al.*[26] are shown in *Figure 4*. Profiles A and B clearly indicate a variation in the relative intensity of the 200 and 110 crystal peaks as a function of the method of polymerization. It is intriguing to note that the authors of references 25 and 26 have attempted to interpret these variations in relative intensity in terms of a third structural component which is held to be nematic or mesomorphic.

Before we go on to consider the nature of crystallinity in PVC it is appropriate to review the ideas of Juijn in rather more detail.

The Juijn proposal

Using CPK models of syndiotactic, isotactic and mixed tacticity oligomers, Juijn determined the way in which isotactic sequences might be incorporated into the crystals comprising syndiotactic chains in the planar zigzag conformation. It is apparent that isotactic units are only able to emulate the syndiotactic planar zigzag shape when they occur in sequence lengths which have even numbers. *Figure 5* shows a CPK model of a syndiotactic PVC chain in planar zigzag conformation ($\phi = 180°$)* with two consecutive isotactic

* In this paper we use 180° to denote the *trans* or planar zigzag conformation, this is opposed to 0° which Juijn used but in keeping with modern day modelling practice. We are following the convention used by the molecular modelling MOPAC method where, for example, torsion angles 155°, 155°, 205°, 205° are expressed as 155°, 155°, −155°, −155°

units substituted at its centre, the central four backbone bonds being set approximately in the Juijn conformation. The efficiency with which the double isotactic defect in this conformation is able to emulate the shape of planar zigzag syndiotactic segments is so good that it can be difficult to distinguish at first sight where the defect is situated (although it is more obvious if the sequences are viewed from the opposite direction so as to show more hydrogen atoms). By close examination of space filling models, Juijn was apparently able to estimate the energy associated with each conformation. He found that the energy of an isotactic conformation emulating a syndiotactic planar zigzag was higher than the minimum energy 3/1 helical conformation by $\sim 4.19\,\mathrm{kJ\,mol^{-1}}$ monomer. A major difficulty in trying to interpret the conformation of the shape-emulating chains, stems from Juijn's use of the three terms: T (*trans*), G_r (*gauche* right) and G_l (*gauche* left) without further definition to describe the conformation of each backbone bond. If, however, one builds models that match his photographs[17,18] then it is immediately apparent that the '*gauche*' must be meant as a distortion from *trans* rather than setting exactly $\pm 120°$ away, despite the latter settings being implied in a Newman projection diagram. Indeed, each torsion angle appears to be rotated from the planar zigzag by $\sim \pm 32°$ (this value was obtained by reading off a graph in the appendix of Juijn's paper and is the only value that he quotes or estimates for the torsion of the backbone in this conformation). Although his studies were based on nothing more complex than CPK (space filling) models, Juijn was the first person to demonstrate the idea of isotactic co-crystallization and that, as a consequence, a crystallinity of 8.5% could be achieved with crystals of 12 monomer units thick through the incorporation of even-numbered isotactic sequences into the otherwise planar zigzag syndiotactic crystals. This value of crystallinity compares favourably with experiment and is in marked contrast to the limit of 0.45% for purely syndiotactic crystals of the same thickness.

Molecular modelling of PVC

While PVC has been examined by several authors using computer-based molecular modelling techniques[29–31], the possibility of shape emulation as in the Juijn model does not appear to have been addressed. Recent treatments using semi-empirical methods[30,31] were found to model isolated chains of PVC effectively, although first level parameters on which most molecular mechanics methods are based remain somewhat inadequate for this type of polar molecule[29].

In this study AM1 parameters have been used within the semi-empirical modelling package known as MOPAC (V), because of their acknowledged reputation for successfully representing the polar interactions of vinyl molecules. At a first stage, two-dimensional rotational energy maps were calculated by setting a neighbouring pair of backbone bonds (chosen with the non-substituted carbon in the centre) to fixed values of torsion angles, ϕ_1 and ϕ_2, in 20° increments. The contour plots of the total energy as functions of ϕ_1 and ϕ_2 are reproduced for the syndiotactic and isotactic dichlorosubstituted pentanes in *Figures 6* and *7*, respectively.

In *Figure 6* (syndiotactic model), there is clearly one minimum energy conformation (shaded). It is close to a planar zigzag, the torsion angles being rotated by $\sim 10°$

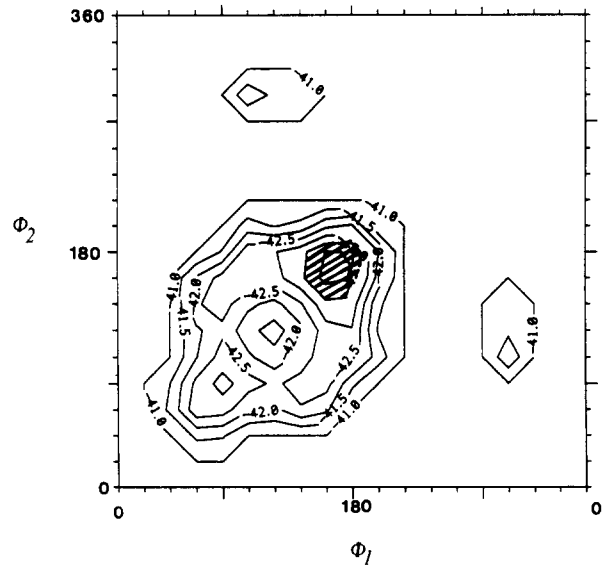

Figure 6 Contour map showing the change in energy as a function of the rotational setting of the two middle bonds in racemic 2,4-dichloropentane (a model for syndiotactic PVC). Rotation is calculated at 20° intervals. The minimum energy region is shaded. Contours are not drawn in for the high energy regions; units of the energy contours are kcal $\mathrm{mol^{-1}}$

from this conformation to 170°, 170°. On the other hand the isotactic map (*Figure 7*) has two conformational energy minima at 70°, 190° and 170°, 290°. These latter torsion angle values correspond approximately to the $\bar{g}t$ and tg conformations, which when repeated along the chain would form left- or right-handed 3/1 helices. The positions of the Juijn conformation (212°, 212° and 158°, 158°) are marked as circled crosses on this map. *Figure 7b* is a higher resolution version of *Figure 7a* which shows that for a two-dimensional (dyad) plot these conformations do not lie in subsidiary minima although they are sited in valleys running up from the low energy regions towards the lower right of the diagram.

While the maps of *Figures 6* and *7* reveal nothing new, they serve as guides to the variation of energy in conformational space and are a useful basis in interpreting the results of the multi-dimensional conformation modelling that follows.

Energy minimization of PVC octamers

The energy cost of an isotactic molecule emulating the shape and axial repeat of a syndiotactic planar zigzag sequence can be determined by utilizing another routine available within MOPAC, specifically designed for polymers. The routine enables the conformation of longer oligomers to be optimized whilst also offering the unique opportunity to either monitor or fix absolutely the end-to-end length of the chain. Polymers are thus represented by oligomers consisting of eight monomer units. The longer range interactions are assessed by using translation vector notation. Unless otherwise stated all geometric variables of the oligomers are optimized, the starting point being conformations comparatively close to those of interest ($\pm 5°$). Since the technique allows the optimization of a conformation to be carried out either on a molecule of fixed length or on one that is free, it has been possible to investigate the energetic consequences of stretching the emulating isotactic conformations to

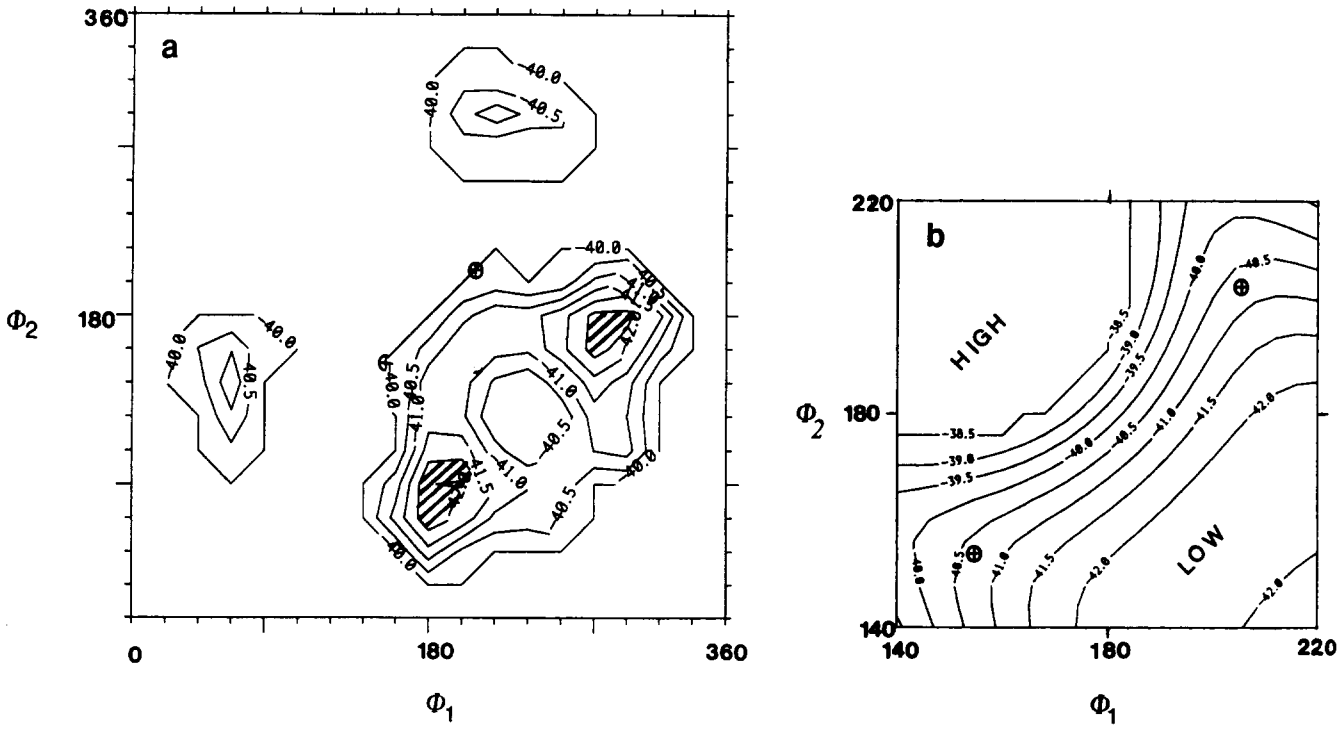

Figure 7 (a) Contour map showing the change in energy as a function of the rotational setting of the two middle bonds in *meso* 2,4-dichloropentane (a model for isotactic PVC). Rotation is calculated at 20° intervals. The minimum energy region is shaded. Contours are not drawn in for the high energy regions; the units of the energy contours are kcal mol^{-1}. (b) An enlarged view of the central region of (a). As before, contours are not drawn in for the high energy regions and the units of the energy contours are kcal mol^{-1}

Table 2 PVC oligomers (eight monomer units); MOPAC (AM1) optimization results

Oligomer (eight monomer units)	Backbone torsion angles (°)	Bond angles (°)	Axial length of oligomer (Å)	Heat of formation (kJ mol^{-1})	$\Delta H_{(conf-min)}$ (kJ mol^{-1} monomer)	Dipole (D)
			No restraints			
Syndiotactic						
Planar zigzag	169, 168 −169, −167	112.5, 111	20.06	−635.20	-	6.63
Isotactic						
3/1 helix	64.5, −178.5	114, 112	16.41	−601.14	-	2.82
Structure emulating shape of syndiotactic planar zigzag	155, 154, −157, −155	116, 109, 115.5, 111.5	20.00	−495.72	13.24	9.98
			End-to-end length of oligomer set at 20.32 Å (to match observed axial repeat in the crystal)			
Syndiotactic						
Planar zigzag	169, 169, −168, −170	113.5, 112.5	20.32	−626.91	1.05	6.76
Isotactic						
Structure emulating shape of syndiotactic planar zigzag	156, 154, −157, −156	117, 111, 117, 113	20.32	−486.46	14.41	10.05

lengths exactly comparable with the syndiotactic planar zigzag.

Data obtained from the energy minimization of the syndiotactic and isotactic PVC octamers are listed in *Table 2*. It is interesting to note that the optimized form of the syndiotactic oligomer is not 180°, 180° but has torsion angles close to 170°, 170° as suggested by the two-dimensional syndiotactic rotational energy contour map (the actual figures average to 168°, 168°). It should be noted that the glide plane relationship of the successive dyads in the syndiotactic molecule still remains intact as the dihedral torsion angles are actually 168°, 168°, −168°, −168°, 168°, 168°, etc. This distortion away from the planar zigzag conformation causes the chlorine atoms to be located slightly further apart from those in the structure proposed by Natta and Corradini[11] and is illustrated in *Figure 8*. A most significant finding is that when the conformation of the isotactic octamer is optimized from anywhere near the emulating conformation (suggested by Juijn to be ±32° away from the planar zigzag), then the molecule is found to stabilize in a subsidiary minimum at 155°, 154°, −157°, −155°,

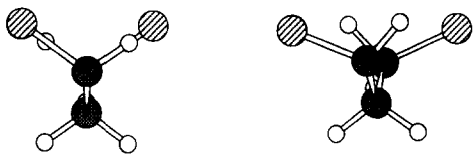

I II

Figure 8 Syndiotactic chains projected onto an *ab* plane: conformation I, assigned from diffraction studies[13] (torsion 180°, 180°); conformation II, predicted by MOPAC (torsion 168°, 168°, −168°, −168°)

in spite of no minimum being observed on the two-dimensional rotational energy contour plot. This is because this isotactic conformation is stabilized by longer range H–Cl interactions than are found in the 2,4-dichloropentane oligomers.

Additionally, the overall length of the molecule of 20.00 Å is not very much less than the predicted length (20.06 Å) of the syndiotactic oligomer (the equivalent crystallographic distance along the *c* axis of the polymer is measured experimentally as 20.32 Å)[13]. The energy of the shape-emulating conformation of the isotactic molecules, although corresponding to a subsidiary minimum in conformational space, is 13.24 kJ mol^{-1} monomer greater than the lowest minimum corresponding to the helix. Although this energy increment is considerably higher than that predicted by Juijn (4.19 kJ mol^{-1})[17,18], it is still lower than the observed[16–18] heat of fusion of PVC* and should not preclude the incorporation of at least a certain proportion of shape-emulating isotactic sequences in the otherwise syndiotactic crystals. In the case of both the shape-emulating isotactic and the syndiotactic models, the amount of energy required to stabilize the conformation when stretched to match the observed axial repeat of 20.32 Å is ~1.05–1.17 kJ mol^{-1} monomer (cf. *Table 2*). It is interesting to note that the imposed extension of ~1.6% is accommodated by the opening out of the bond angles as well as slight changes to the torsion angles.

Molecular modelling thus demonstrates that isotactic PVC has a subsidiary energy minimum in a conformation which closely emulates the shape and repeat distance of the minimum energy syndiotactic planar zigzag conformation.

Modelling of WAXS from PVC

While it has been the similarities between the Van der Waals envelopes of the emulating isotactic conformation and the syndiotactic planar zigzag which have been emphasized so far, the next step is to examine in more detail the differences which are present. Perhaps the most significant is the fact that the chlorine atoms are closer together in the *c* axis projections for the shape-emulating isotactic conformation than those in the syndiotactic planar zigzag, especially if the torsion angles of the latter are distorted to 168°, 168°, −168°, −168° (*Figure 3*). It is thus possible that, if the emulating isotactic sequences were to exist alongside their syndiotactic counterparts in a crystal, the difference in the positions of the chlorine atoms in particular may leave an imprint on the diffraction patterns.

Powder diffraction patterns (for CuKα wavelength) are simulated using CERIUS, a molecular modelling package which originated in this laboratory. *Figure 9* shows the predicted powder patterns for the syndiotactic planar zigzag crystal. Unit cells are based on the data of Natta and Corradini[11] and Wilkes *et al.*[13] in turn, and the profiles, although shifted because of the different lattice parameters, are otherwise compatible. As one would expect, the peak positions are in reasonable agreement with the crystalline component of the experimental data such as shown in *Figure 4*. The widths of the simulated diffraction peaks are chosen to correspond to perfect diffracting crystallites with equivalent dimensions of 100 Å.

If, on the other hand, unit cells are constructed from chains containing different proportions of syndiotactic and isotactic (emulating conformation) monomers, some interesting differences are seen. These structures are generated by substituting the syndiotactic chains in the Wilkes lattice by shape-emulating isotactic sequences (lattices containing 2 × 3 × 2 unit cells). *Figure 10* shows the resulting simulated powder patterns (based on the unit cell and fractional coordinates supplied by Wilkes *et al.*). In addition to the usual 100% syndiotactic unit cell, the crystalline component of the powder patterns of unit cells composed of isotactic chains emulating the syndiotactic planar zigzag conformation as well the 50:50 mixture of the two types of chains have also been calculated. These simulations show that substitution of isotactic sequences into the syndiotactic PVC lattice has a noticeable effect on the diffraction pattern particularly with respect to the relative intensities of the 200 and 110 peaks. In fact, in the case of a unit cell composed of completely isotactic chains in the emulating conformation (not very likely in reality), the ratio of the intensities of the 200 and 110 peaks is the opposite of that seen for the totally syndiotactic polymer.

Extra subsidiary reflections are found in simulations based on unit cells containing mixtures of syndiotactic and isotactic units (note for example the 100 peaks in *Figure 10B*). They are 'superlattice' peaks and arise from

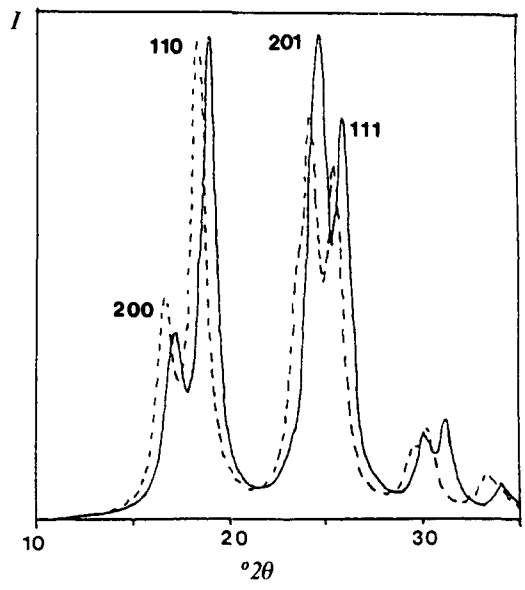

Figure 9 Simulated powder diffraction scans for PVC using: (——) Wilkes *et al.* unit cell parameters[13]; (– – –) Natta and Corradini unit cell parameters[11]

* There is some disagreement in the literature as to the magnitude of the heat of fusion value for PVC, however values of between 2.76 kJ mol^{-1} and 12.65 kJ mol^{-1} have been reported[16–18]

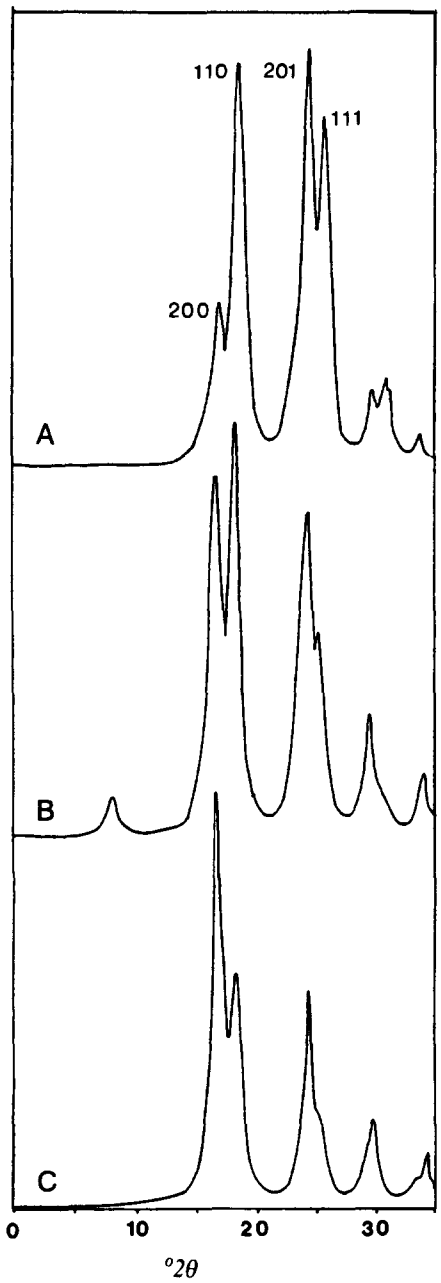

Figure 10 Simulated powder diffraction scans of PVC, for three different isomeric ratios: (A) 100% syndiotactic monomer units; (B) 50% syndiotactic, 50% isotactic; (C) 100% isotactic monomer units. The isotactic units are in the shape-emulating conformation

the use of a model of limited size. In this case a random distribution of different units will not necessarily be reflected in equal numbers being positioned at the unit cell corners as at the centres. By increasing the size of the model used and minimizing as much as possible any degree of order in the relative positions of the two types of monomer units, the impact of the extra reflections on the WAXS simulations can be reduced. In any case their presence does not alter the relative intensities of the four main reflections which are of most interest in this study.

It is noteworthy that the predicted profile for the 50:50 material in *Figure 10* shows the 200 and 110 reflections with nearly equal intensities giving closer agreement with published experimental data (*Figure 4*) than is achieved by the model based totally on syndiotactic chains. It is possible to understand the increasing intensity of the 200 peak with increasing concentrations of the shape-emulating isotactic sequences within the crystal by considering the positions of the chlorine atoms. For the pure syndiotactic crystal the chlorine atoms tend to lie in layers parallel to (100) but with spacing of $a/4$ (cf. *Figure 2*). The contribution to the 200 structure factor is accordingly modest, and most of the observed intensity of the 200 can be attributed to the backbone carbon atoms. In the case of crystals containing isotactic chains in the shape-emulating conformation, the chlorine atoms are closer together in the c projection (*Figure 11*) and thus can be viewed as concentrating more onto layers parallel to (100) with a spacing of $a/2$. It is thus to be expected that the intensities of the 200 is much higher, as is seen.

A plot of the relative intensity of the 200 and 110 peaks determined from the model calculation *versus* the tacticity of those chains which contribute to the crystal is displayed in *Figure 12*. However, while experimental measurements of the 110/200 intensity ratio are available as a function of tacticity, they are not directly comparable with the

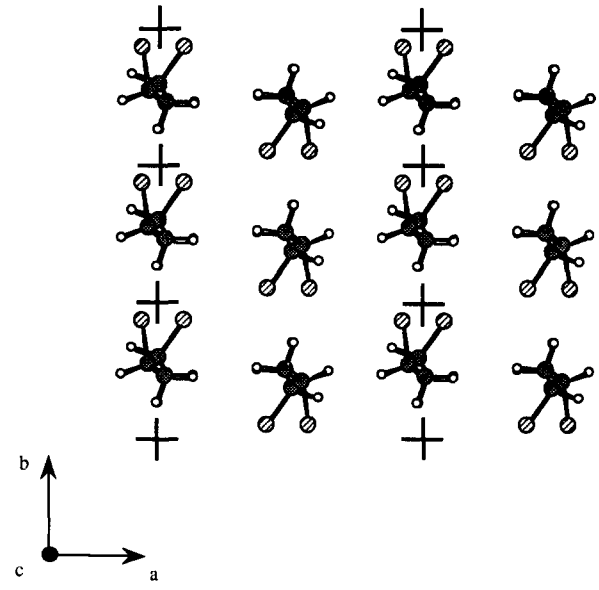

Figure 11 A c axis projection of PVC, on the Wilkes *et al.* lattice constructed from the dimensions given in reference 13, in which the usual syndiotactic units have been substituted by shape-emulating isotactic units

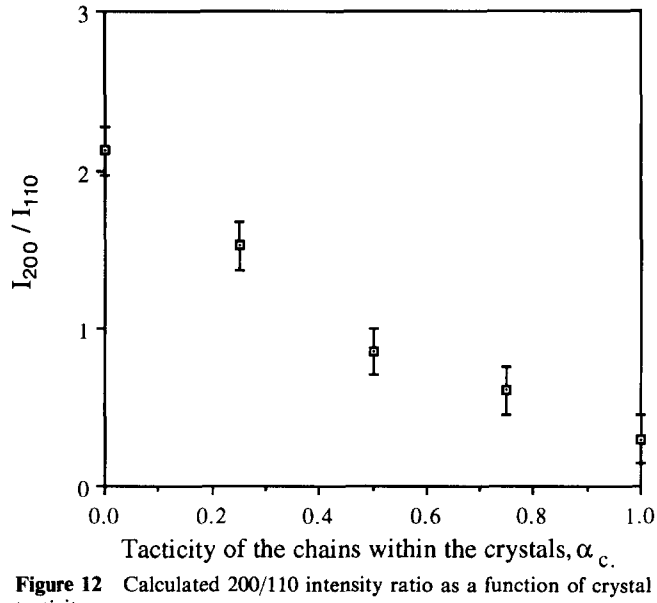

Figure 12 Calculated 200/110 intensity ratio as a function of crystal tacticity

predictions of *Figure 12*, as the measured tacticity (n.m.r.) refers to the overall value for the chains whereas the crystal diffraction is calculated as a function of the tacticity of crystallizable sequences. Thus, if we are to be able to read overall chain tacticity directly from diffraction data it is necessary to understand the relationship between the overall tacticity and that within the crystals.

Tacticity and the nature of the PVC crystallite

The tacticity of a polymer crystallite must depend on those sequences that are excluded or included in a crystallite. In order to calculate the crystallinity which might be expected for a given crystal thickness, it is necessary to calculate the different permutations of crystallizable sequence and their probability.

When we examined the way in which crystallinity has been estimated in the past several interesting points were revealed. Fordham[20] showed that the probability of a crystallizable sequence, P_N, composed of N syndiotactic units, terminated by two isotactic ones, is related to the polymer tacticity (α) by the equation:

$$P_N = N(1-\alpha)^2\alpha^N \quad (1)$$

On a similar basis, Juijn[17,18] derived equation (2) to calculate the fraction of crystallizable sequences of length N which in this case can be seen to consist of syndiotactic units which might contain subsequences of even numbers of isotactic units. Sequences were terminated by sis end defects, i.e. single isotactic isolated units.

$$P_N = (1-\alpha)\alpha^N \sum_{i=0}^{i=N-1/2} \frac{(N-1-i)!}{(N-1-2i)!i!}\left(\frac{1-\alpha}{\alpha}\right)^{2i} \quad (2)$$

It is possible to determine the different types of crystallizable sequence. On close examination of equation (2) it can be seen that not all types of crystallizable sequences are included in the crystallite and, in fact, the amount of crystallinity is underestimated. While equation (1), for purely syndiotactic sequences predicts a maximum crystallinity of 0.272%, for a crystal thickness corresponding to $N=13$ and $\alpha=0.55$, the Juijn method predicts the maximum crystallinity to be 6.88%. This estimate is closer to, although still less than, the experimental crystallinity of $\sim 10\%$[8–10,16] found in polymers which have a dyad tacticity of 0.55.

In the Appendix we critically examine the precepts of the Juijn equation and present a new approach. We first determine the probabilities of a sequence of length N, chosen at random from a chain and *not* being crystallizable on account of containing forbidden sequences such as sis, siiis, etc. In this way the difficult problem of definition of the terminating sequences is avoided, while the possibility of a sequence longer than N contributing to a crystal of thickness N is specifically included*.

Our method predicts the crystallinity of a polymer with $\alpha=0.55$ and with the crystal thickness set at the experimental value of 33 Å ($N=13$), to be of the order of 10.5% which is in good agreement with experimental values. The figure in the Appendix shows that the minimum crystallinity for a crystallizable length, $N=13$, occurs for dyad tacticities between 0.6 and 0.7. While perhaps strange at first sight, this behaviour can be understood if one considers that by far the most influential effect on the crystallite tacticity is the exclusion of all sis defects. Since the exclusion of a sis defect means that two syndiotactic units are excluded for every one isotactic unit, then it is not surprising that the point where the ratio of syndiotactic to isotactic units is two to one is also the point of minimum crystallinity. Juijn's crystallinity values also show this trend. Caution is called for in comparing these predictions of crystallinities as a function of α with experimental values over a range of tacticities, for they have only been calculated for one crystal thickness, that observed experimentally in the $\alpha=0.55$ polymer. We are not aware of any thickness measurements made on higher tacticity samples of PVC.

Comparison of predicted and experimental intensity ratios

The statistical treatment also enables the tacticity of the crystallizable sequences, α_{cryst}, to be determined as a function of the overall tacticity, α. The results, which are not dependent on N, are plotted in *Figure 13*. Note that the tacticity of a crystallite is observed to rise with increasing tacticity of the whole polymer and although the relationship is not linear, the two tacticity values are related closely enough to indicate that, in addition to defining the crystallites, the 200/110 ratio might also be a useful indicator of the overall polymer tacticity.

The relationship plotted in *Figure 13* enables us to compare experimental measurements of peak intensity ratio with those predicted by diffraction modelling. While many diffraction scans have been published, mostly for tacticities around 0.55 and 0.68 as measured by n.m.r., comparatively few are presented in such a way to enable us to measure the 110/200 ratio with some confidence. We have thus chosen the data of Guerrero *et al.*[26], for

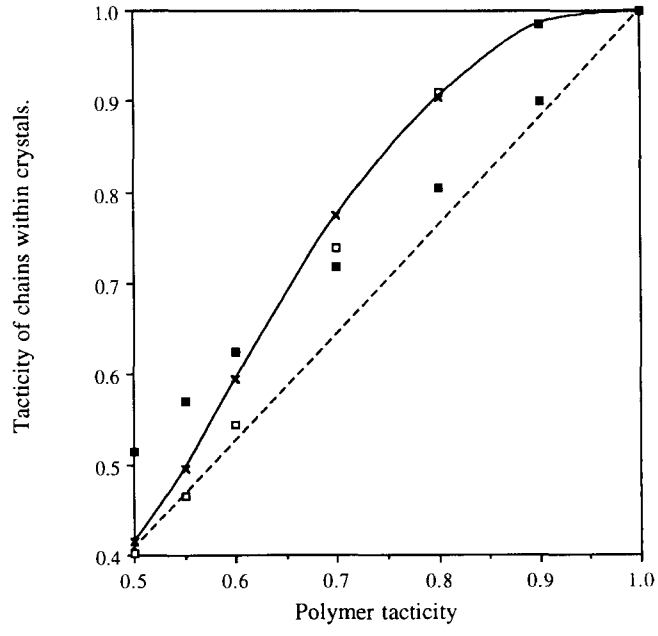

Figure 13 Tacticity of chains within the crystals plotted against polymer tacticity: (□) tacticity of chains with sis units excluded; (■) tacticity of chains with siiis units excluded; (×) α_c, tacticity in crystals with all forbidden sequences excluded

* There is a problem in taking out sis units in the manner described in the Appendix. While compensation is properly made for the change in composition of the chain, we have assumed that the distribution of the units in the chain is still random. We acknowledge this as an approximation. Comparison with more recent computer calculations which generate all possible sequences for a given length has shown that the above approximation leads to an underestimation in the crystallinity by 1 or 2%

comparison with predictions for they combine clear diffraction scans, which are necessary for the measurement of the amorphous background, with n.m.r. measurements of overall tacticity which fall at the centre of the published range of values for the polymerization conditions used.

The experimental values of I_{200}/I_{110} as a function of α_c (determined from α using *Figure 13*) are plotted together with the predicted intensity ratios in *Figure 14*. The agreement is encouraging and provides additional confirmation that the prime cause of the changing intensity ratio with tacticity is the incorporation of shape-emulating isotactic sequences within the otherwise syndiotactic crystals.

Thermal properties

It is well established that the melting point of PVC rises with increasing syndiotacticity. This is illustrated in *Figure 15* (drawn using data from reference 32). The dyad tacticity range corresponding to a polymerization temperature of −75°C to 125°C should be from 0.68 to 0.50 (as measured by n.m.r.). While the straightforward explanation of such a trend is in terms of reduced tacticity leading to smaller crystal thicknesses and thus lower melting temperatures, the variation from 155 to ~320°C over a comparatively modest tacticity range is certainly large. For a material with a syndiotactic dyad concentration of 0.55, the crystal thickness has been measured to be ~33 Å. Further increases in thickness with syndiotacticity could account for the observed increase in melting point, but would suggest a strangely high surface energy at least for this polymer. It is thus especially attractive to associate the large dependence of melting point on tacticity with the incorporation of shape-emulating isotactic sequences into the crystals. We have a value, from modelling, for the excess energy associated with such defects to be 13.24 kJ mol^{-1}. In trying to assess the influence of a concentration of such defects on the melting point we need to know the heat of melting (ΔH) for a syndiotactic crystal. Such values are not available for polymeric material and the measurement of ΔH for samples of intermediate tacticity gives values[16–18] scattered over a wide range from 2.76 to 12.65 kJ mol^{-1}. Dawson *et al.*[28] considered the main source of error to be the necessary, parallel determinations of crystallinity. While not wishing to enter any debate over the reliability of widely differing sets of reported data, it is worth pointing out that a crystal with a tacticity of 0.55 would be expected to have, on account of the included isotactic units, a $\Delta H_{melting}$ at least 6 kJ mol^{-1} less than that of the pure syndiotactic material. Given the general band of reported values up 12 kJ mol^{-1}, there must be every expectation that the incorporation of isotactic units or sequences will have a pronounced influence on reducing the melting point. The observed steep variation of melting point with tacticity is thus commensurate with the crystal model of included, shape-emulating isotactic sequences.

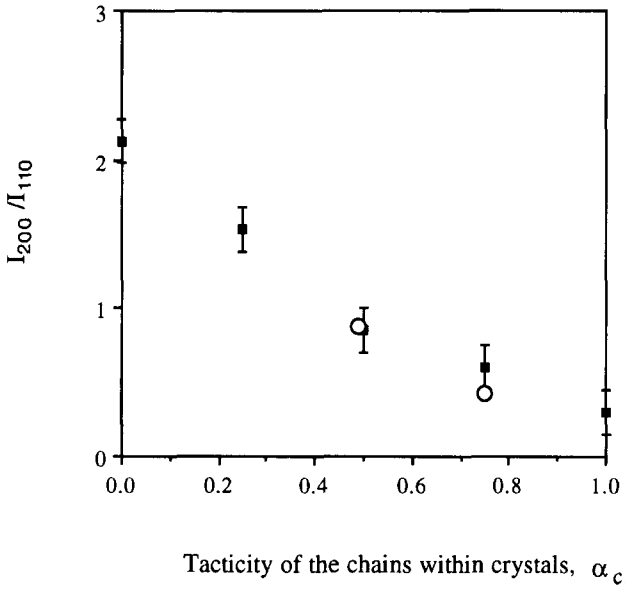

Figure 14 Comparison of the simulated intensity ratio (■) with 200/110 experimental values (○) derived from *Figure 4* (*Table 3*)

Table 3 Experimental values of the intensity ratio, I_{200}/I_{110}, as a function of polymer tacticity (*Figure 3*[26]). The table also includes computed values of the crystal tacticity (α_c) as determined from *Figure 13*

Polymerization conditions	α	I_{200}/I_{110}	α_c
Emulsion (room temperature)	0.55	0.875	0.495
Polymerized in n-butyraldehyde	0.68	0.43	0.75

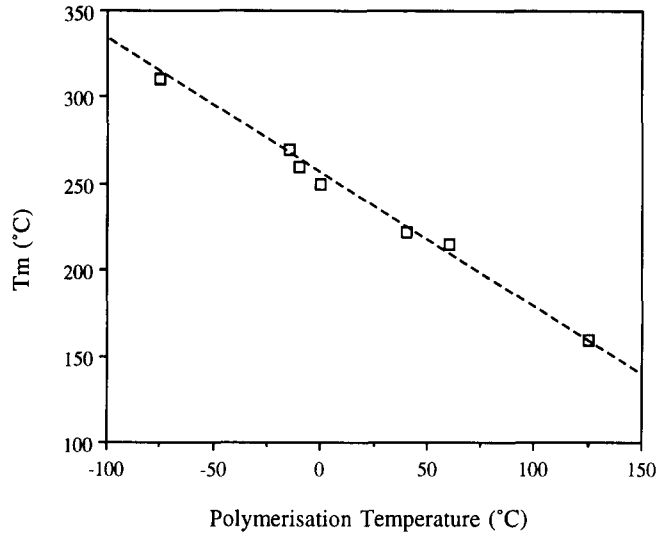

Figure 15 Effect of polymerization temperature on the melting point of PVC (data taken from reference 32)

POLYACRYLONITRILE

Comparison with another related vinyl polymer

The idea that certain isotactic sequences of PVC may emulate the shape of a syndiotactic chain and thus take part in crystallization opens up the question of generality. Could, for instance, similar co-crystals exist in other vinyl polymers, particularly those that are highly polar? In taking up this issue, we have extended our modelling approach to the chain conformation of another commercially important polymer, PAN.

Polyacrylonitrile

PAN is similar to PVC in that the polarity and size of the side groups are comparable. Both crystal lattices are orthorhombic and have similar dimensions (see *Table 1* for lattice parameters of PVC and *Table 4* for lattice parameters of PAN), but whereas the PVC

Table 4 Unit cell dimensions for crystalline PAN

Reference	*a* (Å)	*b* (Å)	*c* (Å)	System
Syndiotactic				
37	5.99	5.99	–	Hexagonal
38	21.18	11.60	(5.1)	Orthorhombic
39	10.6	11.6	5.04	Orthorhombic
40	10.2	6.1	5.1	Orthorhombic
41	10.55	5.8	5.08	Orthorhombic
42	21.0	11.9	5.04	Orthorhombic
43	10.7	12.1	(5.1)	Orthorhombic
Isotactic				
44	4.74	4.74	2.55	Tetragonal

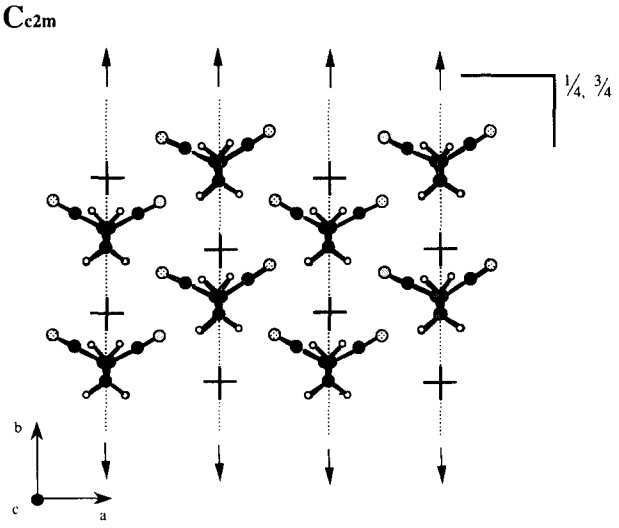

Figure 16 Crystal structure of PAN, where the chains are arranged as suggested by Stefani *et al.*[40] but on the lattice proposed by Holland *et al.*[41]

lattice has the symmetry according to the space group P_{cam}, PAN has the space group C_{mc2}. (As drawn in *Figure 16* it appears the space group is actually Cc2m.) Representations of both structures can be found in *Figures 2* and *16*. The crystal structures differ because in PAN all chains have the same rotational settings, the substituted groups being on the same side, whereas in PVC every alternate molecule is rotated by π about its chain axis.

As with PVC, the degree of crystallinity in PAN is substantially greater than that predicted from the tacticity (indeed it has been reported as high as 28–34% for the 40% syndiotactic polymer)[39] and authors have sought to explain the high crystallinity in terms of PAN having only lateral order[33] or paracrystalline order[34]. The dyad tacticity of PAN also suggests that there are more isotactic units present than syndiotactic monomer units[32]. Although studies[35,36] have been performed to try and identify the extra crystalline element, a convincing explanation has remained elusive. As the conformation of crystallizable sequences of syndiotactic PAN is planar zigzag, there is reason to suppose that, like PVC, the amount of crystallinity in PAN is enhanced by the ability of isotactic sequences to emulate the shape of the syndiotactic planar zigzag molecules. In order to explore this possibility, the conformational structures of PAN chains have been investigated by molecular modelling too, and, as with PVC, the corresponding X-ray powder patterns simulated.

Molecular modelling of PAN

Figures 17 and *18* are two-dimensional rotational energy contour maps for syndiotactic and isotactic PAN. These were calculated for disubstituted pentane model compounds using the computer modelling program MOPAC by simulating the change in energy as rotation is applied to neighbouring bonds.

The map for syndiotactic PAN is extremely similar to the one calculated for syndiotactic PVC, with the global minimum again at 170°, 170°. On the energy map of isotactic PAN in *Figure 18*, two small crosses mark the torsion angles of the Juijn conformation. As far as can be judged there are few if any differences between the PVC and PAN profiles in the areas marked.

Energy minimization of PAN octamers

The results from the energy minimization of isotactic and syndiotactic octamer chains of PAN are presented in *Table 5*. Column 2 lists the backbone torsion angles and column 4, the energy associated with these conformations. The results in *Table 5* confirm the observation drawn from the energy map that for the syndiotactic molecule the all-*trans* conformation is not 180° but off set by ~13–14°, a deviation larger than that seen in PVC (11–12°). Conversely, the torsion angles of the isotactic shape-emulating conformation are off set from the planar zigzag by 20°, a smaller amount than for PVC (28°). In addition, the extent of opening and closing of the backbone bond angles in PAN is significantly less than in PVC.

The molecular modelling of PAN shows that not as much energy (12.53 kJ mol^{-1} monomer, cf. 14.33 kJ mol^{-1} monomer for PVC) is required to form the shape-emulating structure in the isotactic chain compared with a 3/1 helix.

For PAN, the analysis of the WAXS to determine the *c* axis repeat is difficult. Holland *et al.*[41] managed to obtain a value identical to that seen for PVC[8–10].

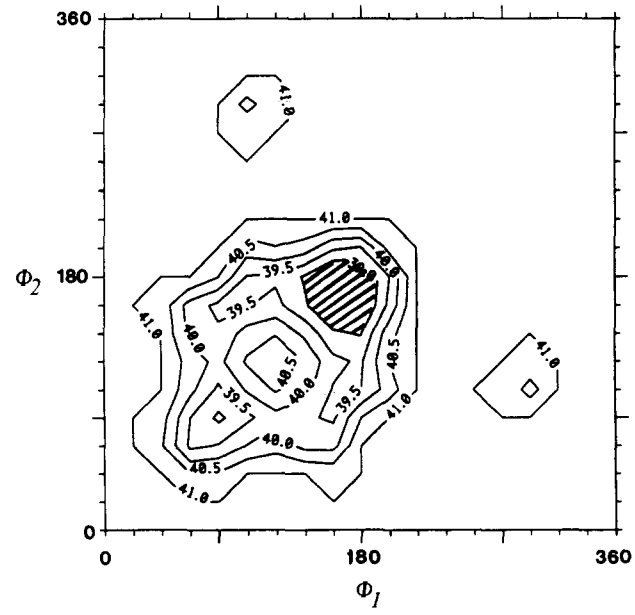

Figure 17 Contour map showing the change in energy as a function of the rotational setting of the two central bonds in racemic 2,4-dicyanopentane (a model for syndiotactic PAN). Rotation is calculated at 20° intervals. The minimum energy region is shaded. Contours are not drawn in for the high energy regions; the units of the energy contours are kcal mol^{-1}

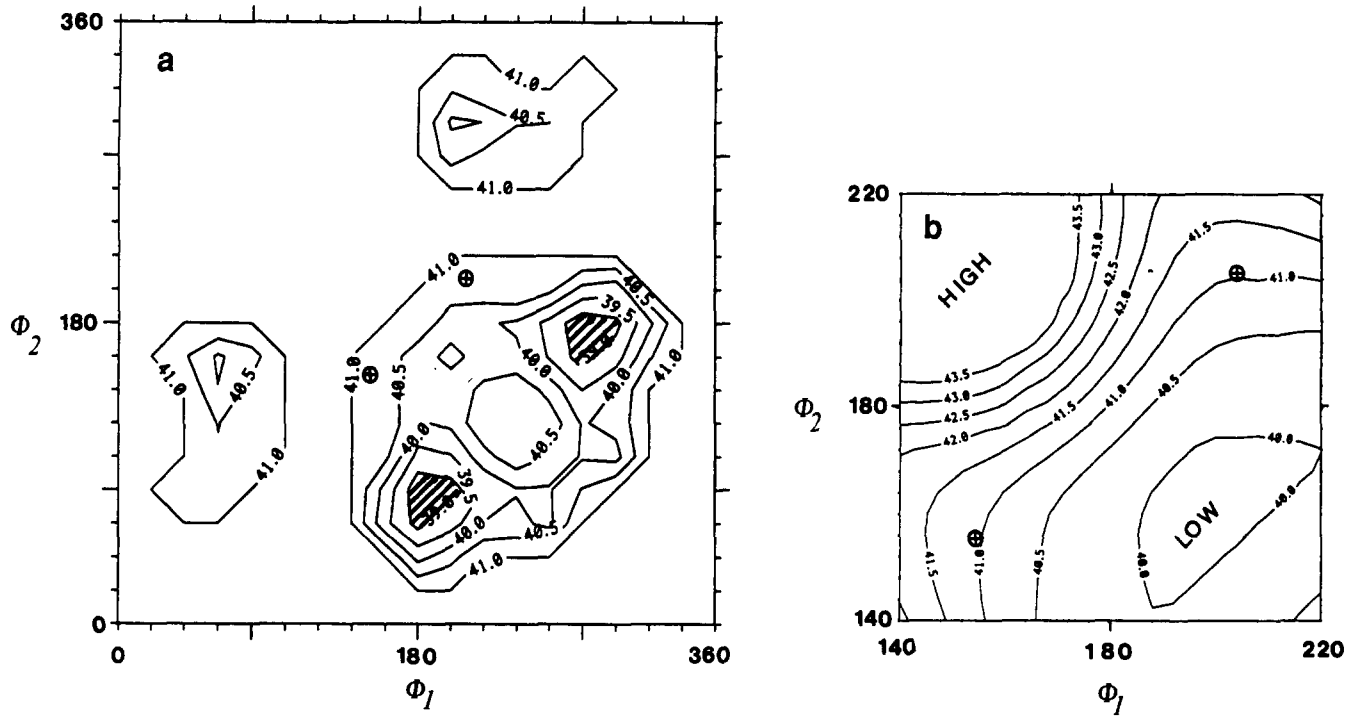

Figure 18 (a) Contour map showing the change in energy as a function of the rotational setting of the two central bonds in *meso* 2,4-dicyanopentane (a model for isotactic PAN). Rotation is calculated at 20° intervals. The minimum energy region is shaded. Contours are not drawn in for the high energy regions; the units of the energy contours are kcal mol^{-1}. (b) An enlarged view of the central region of (a). As before, contours are not drawn in for the high energy regions and the units of the energy contours are kcal mol^{-1}

Table 5 PAN oligomers (eight monomer units); MOPAC (AM1) optimization results

Oligomer (eight monomer units)	Backbone torsion angles (°)	Bond angles (°)	Axial length of oligomer (Å)	Heat of formation (kJ mol^{-1})	$\Delta H_{(conf-min)}$ (kJ mol^{-1} monomer)	Dipole (D)
			No restraints			
Syndiotactic						
Planar zigzag	167, 166. −167, −167	112, 111	20.10	734.38	–	10.55
Isotactic						
Helix	77.5, −173	111, 112.5	16.18	743.52	–	4.72
Structure emulating shape of syndiotactic planar zigzag	161, 160, −162, −159	113.5, 110	20.10	837.41	11.73	18.25
			End-to-end length of oligomer set at 20.32 Å (to match observed axial repeat in the crystal)			
Syndiotactic						
Planar zigzag	168, 168, −168, −168	113, 112	20.32	739.54	0.63	10.76
Isotactic						
Structure emulating shape of syndiotactic planar zigzag	162, 159, −162, −160	114, 111, 114, 110	20.32	843.61	12.53	18.31

Comparison of this length with that of the octamers reveals four important points: first, that MOPAC predicts the syndiotactic and shape-emulating isotactic oligomer to have the same length, second, that this distance is very close to the equivalent crystallographic distance for this oligomer length, third, that they are marginally longer than the same PVC oligomers and finally that the extra cost in stretching the two different oligomers to the exact crystallographic distance is ~0.63–0.80 kJ mol^{-1} monomer. There is therefore strong justification for the view that isotactic sequences in otherwise syndiotactic PAN chains can also form shape-emulating conformations.

Modelling of PAN diffraction

Very much in the same manner to the PVC simulations, and using the unit cell parameters of Holland *et al.*, WAXS profiles were simulated for PAN for different tacticities (*Figure 19*). As with PVC, the simulations were based on lateral crystallite dimensions of 100 Å × 100 Å, although the peak breadth associated with the poor longitudinal register between the molecules was allowed

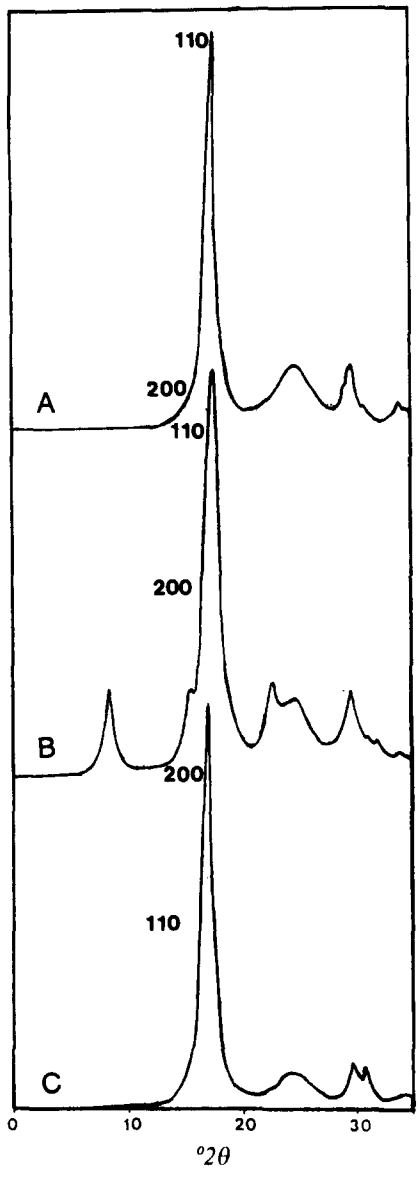

Figure 19 Simulation of powder diffraction scans of PAN, for three different isomer ratios: (A) 100% syndiotactic monomer units; (B) 50% syndiotactic, 50% isotactic; (C) 100% isotactic monomer units (no long range *c* axis order). The predicted intensity of the 110 and 200 components of the main peaks are as indicated by the vertical positions of the indices

for by selecting an 'apparent' crystal size in the chain direction of 10 Å.

WAXS was simulated for each of the unit cells found in *Table 4* and, not surprisingly, the orthorhombic structures were found to be so close to the hexagonal ($a/b \approx \sqrt{3}$) structure that the 200 and 110 peaks are superimposed in each case. In PVC, the simulations indicated that the relative intensities of the 200 and 110 peaks change with tacticity. The same was also seen in the simulations of PAN in *Figure 19*, although the intrinsic broadness of the overlapping peaks means that it is difficult to resolve the relative intensities experimentally.

Our WAXS simulations have been based on the parameters of Holland *et al.*[41] and in most cases these parameters are very similar to others that are listed in *Table 4*. Note also that large unit cells, which are multiples of the Holland lattice, have also been reported on the basis of diffraction studies of PAN[38,39,42,43]. In each case, the assignment of a larger unit cell is associated with the observation of additional reflections at lower angles. It is significant that these 'superlattice' reflections, which give rise to a doubling of the unit cell parameters, are apparent in our simulations of isomerically mixed crystals (e.g. 50:50; *Figures 11* and *19*) of PVC as well as of PAN. They are associated with less than random packing distributions of the different sequences in the chains. It appears that experimental observations of such low angle peaks, while providing evidence for the non-random packing of sequences, are in themselves further confirmation of the presence of shape-emulating isotactic sequences in the otherwise syndiotactic crystals.

CONCLUSIONS

1. Molecular modelling calculations on model octamers of both isotactic PVC and isotactic PAN show a subsidiary energy minimum close to the conformation first indicated by Juijn[17,18].
2. This conformation enables the isotactic sequences to emulate the general shape and axial repeat of the syndiotactic planar zigzag, and for even numbered runs of isotactic units, provides the means of co-crystallization of such isomerically mixed chains.
3. A statistical approach, in which the probability of forbidden sequences such as sis *not* being present in a randomly chosen section of chain is calculated, provides a relationship between the overall tacticity of the polymer and the tacticity of the crystalline component. It is clear that the incorporation of shape-emulating isotactic sequences enables crystals to exist which have a low tacticity which is not very different from that of the polymer as a whole.
4. The incorporation of shape-emulating isotactic sequences into the crystals of PVC is able to account, quite precisely, for the experimentally observed combinations of crystallinity and crystal thickness (10% and 33 Å) seen in commercial atactic ($\alpha = 0.55$) polymer. At the same time it provides a qualitative explanation of the even higher crystallinities observed in atactic PAN.
5. Diffraction modelling of PVC crystals containing different proportions of syndiotactic and shape-emulating isotactic sequences, predicts a significant variation in the relative intensities of the 200 and 110 diffraction peaks as a function of crystallite tacticity. This prediction is in accord with well established experimental observations, which have not previously been explained in terms of crystal diffraction and thus now provide direct evidence for the incorporation of shape-emulating isotactic sequences into the otherwise syndiotactic crystallites.
6. The relative intensities of the same diffraction peaks from PAN crystallites is similarly predicted to vary with tacticity. The fact that the chain packing in PAN is close to being hexagonal means that the two peaks are often superimposed in experimental data and are difficult to resolve.
7. Predicted crystal diffraction patterns of both PVC and PAN show low angle peaks for mixed isomeric compositions which are associated with a non-random packing distribution of the syndiotactic and shape-emulating isotactic sequences (difficult to avoid with small models). Such peaks have been observed experimentally in both polymers where they lead to the identification of unit cells with doubled lattice

parameters. They thus provide further evidence for the presence of mixed isomer crystallites.

ACKNOWLEDGEMENTS

The authors would like to thank Professor C. J. Humphries for the provision of laboratory facilities and Professor A. Keller, Dr S. Hanna, Dr P. J. Withers and our friends at Molecular Simulations Ltd (Cambridge) for helpful discussions. The work was funded by 3M and we are grateful to Dr S. P. Birkeland and Dr A. G. Hulme-Lowe for their encouragement and support.

REFERENCES

1 Flory, P. J. *Trans. Faraday Soc.* 1955, **51**, 848
2 Windle, A. H., Viney, C., Golombok, R., Donald, A. and Mitchell, G. *Trans. Faraday Soc.* 1985, **79**, 55
3 Lemmon, T., Hanna, S. and Windle, A. H. *Polym. Commun.* 1989, **30**, 2
4 Chivers, R. A., Blackwell, J., Gutierrez, J., Stamatoff, J. B. and Yoon, H. 'Polymeric Liquid Crystals' (Ed. A. Blumstein), Plenum Press, New York, 1985
5 Lovell, R. and Windle, A. H. *Polymer* 1981, **22**, 175
6 Cavalli, L., Borsini, G. C., Carraro, G. and Confalonieri, G. *J. Polym. Sci. A1* 1970, **8**, 801
7 Pham, Q. T., Millan, J. and Madruga, E. L. *Makromol. Chem.* 1974, **175**, 945
8 Repko, E., Tureckova, M. and Halamek, J. *Petremia* 1966, **14**, 25
9 Garbuglio, G., Rodella, A., Borsini, G. C. and Gallinella, E. *Chim. Ind.* 1964, **46**, 166
10 D'Amato, R. J. and Strella, S. *Appl. Polym. Symp.* 1969, **8**, 275
11 Natta, G. and Corradini, P. *J. Polym. Sci.* 1956, **20**, 251
12 Kockott, D. *Kolloid Z. Z. Polym.* 1964, **198**, 17
13 Wilkes, C. E., Folt, V. L. and Krimm, S. *Macromolecules* 1977, **6**, 235
14 Burleigh, P. H. *J. Am. Chem. Soc.* 1960, **82**, 749
15 Nakajima, A. and Hayashi, S. *Kolloid Z. Z. Polym.* 1969, **229**, 12
16 Nakajima, A., Hamada, H. and Hayashi, S. *Makromol. Chem.* 1966, **95**, 40
17 Juijn, J. A. *PhD Thesis* Technical University Delft, 1972
18 Juijn, J. A., Gisolf, G. H. and de Jong, W. A. *Kolloid Z. Z. Polym.* 1973, **251**, 465
19 Lemstra, P. J., Keller, A. and Cudby, M. *J. Polym. Sci., Polym. Phys. Edn* 1978, **16**, 1507
20 Fordham, J. W. L. *J. Polym. Sci.* 1959, **39**, 321
21 Keller, A. *Polym. Sci. Technol.* 1983, **22**, 25
22 Lemstra, P., Keller, A. and Cudby, M. *J. Polym. Sci., Polym. Phys. Edn* 1978, **14**, 39
23 Guerrero, S. J., Keller, A., Soni, P. and Geil, P. H. *J. Polym. Sci., Polym. Phys. Edn* 1980, **18**, 1533
24 Keller, A. personal communication, 1992
25 Mammi, M. and Nardi, V. *Nature* 1963, **199**, 247
26 Guerrero, S. J., Veloso, H. and Randon, E. *Polymer* 1990, **31**, 1615
27 Biais, R., Geny, C., Mordini, C. and Carrega, M. *Br. Polym. J.* 1980, **12**, 179
28 Dawson, P. C., Gilbert, M. and Maddams, W. F. *J. Polym. Sci. B* 1991, **29**, 1407
29 Boyd, R. H. and Kesner, J. *Polym. Sci., Polym. Phys. Edn* 1981, **19**, 375
30 Burdas, J. and Lukas, R. *Makromol. Chem., Macromol. Symp.* 1989, **29**, 321
31 Alig, I., Lochman, R. and Wartewig, S. *J. Polym. Sci., Polym. Phys. Edn* 1984, **22**, 1097
32 Brandrup, J. and Immergut, E. H. (Eds) 'Polymer Handbook', 3rd Edn, Wiley Interscience, New York, 1991
33 Bohn, C. R., Schaefgen, J. R. and Statton, W. O. *J. Polym. Sci.* 1961, **55**, 531
34 Lindenmeyer, P. H. and Hoseman, R. *J. Appl. Phys.* 1963, **34**, 42
35 Ganster, J., Fink, H.-P. and Zenke, I. *Polymer* 1991, **32**, 1566
36 Grobelny, J., Sokól, M. and Turksa, E. *Polymer* 1984, **25**, 1415
37 Natta, G., Mazzanti, G. and Corradini, P. *Atti. Accad. Nazl. Lince., Cl. Sci. Fis., Mat. Nat. Rend.* 1958, **25**, 3
38 Klement, J. J. and Geil, P. H. *J. Polym. Sci. A2* 1968, **6**, 1381
39 Hinrichsen, G. and Orth, H. *Kolloid Z. Z. Polym.* 1971, **247**, 844
40 Stefani, R., Cherreton, M., Garnier, M. and Eyraud, C. *Compt. Rend.* 1960, **251**, 2174
41 Holland, V., Mitchell, S., Hunter, W. and Lindenmeyer, P. *J. Polym. Sci.* 1962, **62**, 145
42 Kumamaru, F., Kajiymama, T. and Takayanagi, M. *J. Cryst. Growth* 1980, **48**, 202
43 Yamazaki, H., Kajita, S. and Kamide, K. *Polym. J.* 1987, **19**, 995
44 Colvin, B. G. and Storr, P. *Eur. Polym. J.* 1974, **10**, 377

APPENDIX

Calculation of crystallinity in PVC

While Fordham[20] defines a crystallizable chain as a sequence of syndiotactic units bound by two isotactic terminating units, Juijn[18] determines the probability of a crystallizable sequence (composed of both syndiotactic and shape-emulating isotactic units) by considering the various different permutations of crystallizable sequence bound by two sis terminating defects. It is clear in the first method that only an isotactic unit will terminate a crystallizable sequence or, if located in the middle of a sequence, will render it non-crystallizable. In Juijn's method, a sequence may be rendered non-crystallizable by the inclusion of a sis unit or in fact any number of odd numbered isotactic units bound by two syndiotactic units, but for some reason it seems only sis units are considered terminating defects. This aspect of the treatment means that, although Juijn's crystallinity values are quite close to those reported experimentally, they are bound to be underestimated.

Definition of chain termination where both syndiotactic and isotactic units are part of the crystallizable sequence is an exceedingly complex problem. For instance, if an odd numbered run of isotactic units of length N is bound by two syndiotactic units then this type of sequence is totally ignored by Juijn's method, even though the chain is of sufficient length to crystallize. For this reason, there are advantages in determining instead the probability of a sequence of length N (corresponding to a particular crystal thickness) that contains any subsequence of the type sis, siiis, etc, and from this determining the proportion of crystallizable sequences.

Starting with the sis defect, the probability of *not* having a sis triad in any of the $N/3$ positions (1,2,3; 4,5,6; 6,7,8; etc., i.e. in positions which do not overlap) is as follows:

$$P'_{\mathrm{sis}} = (1-\alpha^2(1-\alpha))^M \qquad \text{(A1)}$$

where $M = N/3$ (rounded down to the nearest integer).

The next step is to consider the probabilities of there being no overlapping sis triads in the positions 2,3,4; 5,6,7; 8,9,10; etc. Since we are concerned with the probability of there being *no* sis triad in the position 1,2,3 *and* none in the position 2,3,4 (*and* none in 3,4,5 — see below), it is necessary to consider the probability of sis in 2,3,4 with the effective necessity of these sites having been skewed by the absence of sis from 1,2,3 and 4,5,6.

The tacticities of individual triad sites for the first overlap rank are defined as α_{10a}, α_{10b}, α_{10c}. Since effectively $\alpha^2(1-\alpha)$**i** units are missing from position 2, the number present is reduced from $(1-\alpha)$ by this amount. Renormalizing by $1-\alpha^2(1-\alpha)$ gives the new probability for **i** being present and the necessary α, as 1 minus this value, as in equation (A2).

$$\alpha_{10a} = 1 - \left[\frac{(1-\alpha)-\alpha^2(1-\alpha)}{1-\alpha^2(1-\alpha)}\right] \qquad \text{(A2)}$$

Similarly equations can be derived for α_{10b} and α_{10c} but this time the probability of α is directly affected.

$$\alpha_{10b}=\left[\frac{\alpha-\alpha^2(1-\alpha)}{1-\alpha^2(1-\alpha)}\right] \quad \text{(A3)}$$

and $\alpha_{10b}=\alpha_{10c}$.

The probability of not having a sis defect in the first overlap rank is therefore now: one minus the new probability of a defect.

$$P''_{\text{sis}}[1-\alpha_{10a}\alpha_{10c}(1-\alpha_{10b})]^{M_1} \quad \text{(A4)}$$

where $M_1=M-1$ if $N/3$ is an integer and $M_1=M$ if not.

Treatment of the second overlap rank is the same as for the first, except that new values of α_{10a}, α_{10b}, α_{10c} are fed into the equations instead of α and α_{20a}, α_{20b}, α_{20c} to determine P'''_{sis} (taking into account whether $N/3$ has a second remainder or not).

Using these equations, the probability of not having a sis defect in a sequence of length N was ascertained from equation (A5) for a range of initial chain tacticity values. These may be found in *Table A1*, calculated for $N=13$.

$$P_{\text{sis}}=P'_{\text{sis}}P''_{\text{sis}}P'''_{\text{sis}} \quad \text{(A5)}$$

In addition to the sis defect, the probability of *not* having siiis defects (P_{siiis}) has been calculated by a similar method and the values appear in *Table A1*.

The change in tacticity as a consequence of the removal of sequences containing siiiiis defects is very small indeed, so P_{siiiiis} is simply determined from the '1st rank' equation (to the power of $N-6$):

$$P'_{\text{siiiiis}}=[1-\alpha^2(1-\alpha)^5]^{N-6} \quad \text{(A6)}$$

The probability of all defects (in the 0.5–1 tacticity range) equal to or longer than siiiiiiis are so small that they are taken as zero.

Table A1 Calculation of the proportion of crystallizable chains, P_{cryst}, for a thickness of 33 Å. P_{cryst} includes the possibility that a crystallizable sequence of twice the crystal thickness may fold and thus contribute twice. The probabilities of specific 'defect' sequences being absent from the crystal, used in the calculation of P_{cryst}, are listed

	Polymer tacticity					
	0.5	0.55	0.6	0.7	0.8	0.9
P_{cryst}	0.1298	0.1067	0.0886	0.0796	0.1256	0.3285
$P_{\text{cryst}(2N+4)}$	0.0086	0.0080	0.0064	0.0080	0.0188	0.0919
$P_{\text{cryst(tot)}}$	0.1384	0.1147	0.0950	0.0876	0.1444	0.4204
P'_{sis}	$(0.875)^4$	$(0.8639)^4$	$(0.856)^4$	$(0.853)^4$	$(0.872)^4$	$(0.919)^4$
P''_{sis}	$(0.8600)^4$	$(0.8411)^4$	$(0.8255)^4$	$(0.8219)^4$	$(0.8378)^4$	$(0.9050)^4$
P'''_{sis}	$(0.8339)^3$	$(0.7996)^3$	$(0.7671)^3$	$(0.7311)^3$	$(0.7730)^3$	$(0.8843)^3$
P_{sis}	0.1859	0.1425	0.1125	0.0903	0.1316	0.3310
P_{siiis}	0.7375	0.7712	0.8080	0.8890	0.9559	0.9927
P_{siiiiis}	0.9466	0.9616	0.9745	0.9917	0.9986	0.9999

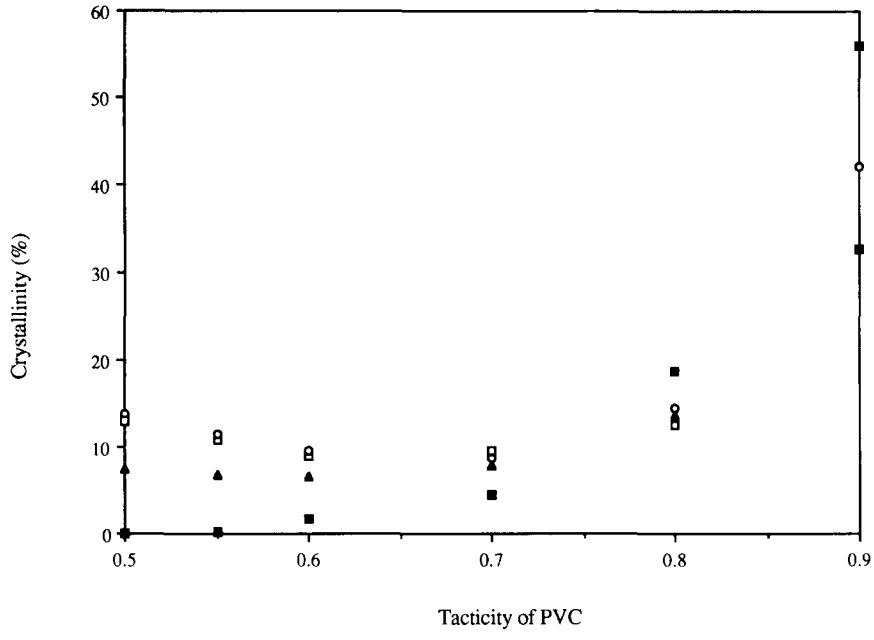

Figure A1 Predicted crystallinity as a function of tacticity: (□) for crystals 33 Å thick ($N=13$); (○) for crystals 33 Å thick but allowing for the fact that crystallizable sequences longer than $2N+4$ might fold; (▲) Juijn's calculations; (■) Fordham's calculations based on the premise that only syndiotactic sequences are crystallizable

The probability of a crystallizable sequence of length N is therefore the product of the probability of not finding a **sis**, a **siiis** *and* a **siiiiis** defect.

$$P_{cryst} = (P_{sis} P_{siiis} P_{siiiiis}) \quad \text{(A7)}$$

Another aspect to consider stems from the fact that, although the crystallizable sequences have to be of length N, they might be indeed longer. Accordingly a crystallizable length may be of the order of $2N + X$ (where X is the estimated number of repeats necessary for the fold and is estimated to be 4). Not surprisingly, this contribution is only significant at higher tacticity and is recorded in *Table A1* and shown in *Figure A1*.

Figure A1 is a plot of the calculated value of P_{cryst} as a function of chain tacticity, for crystal thicknesses of 13 monomer units. It should be emphasized that this value of N is used since it is the value determined experimentally for $\alpha = 0.55$ material. Therefore although this figure can be taken as a good basis for examining the predicted behaviour of the model and comparing that with the predictions of other models if $\alpha = 0.55$, it does not necessarily give a meaningful value for crystallinity, if $\alpha > 0.55$.

It is interesting to note that P_{cryst} at first decreases with increasing tacticity, to reach a minimum between $\alpha = 0.6$ and 0.7, before increasing rapidly at high tacticities. This prediction is a consequence of the fact that the majority of the non-crystallizable, and thus excluded, subsequences are **sis**, and these will be most common when the overall ratio of s to i units is of the order of 2/1. The corresponding plot from Fordham, is of course very much lower as it does not include the possibility of included isotactic units within the crystal. The agreement with Juijn's predictions is quite close, although the current analysis leads to the prediction of a higher crystallinity in region of $\alpha = 0.55$ (the only value of tacticity for which the chosen value of $N = 13$ has any basis) and, as is previously stated, this difference stems from his lack of consideration of other types of terminating end defects such as **siiis**, **siiiiis**, etc.

Calculation of crystallite tacticity

In calculating the crystallinity by the above method it is necessary to consider the tacticity of the individual sites as a function of the rank. If, for the **sis** defect, we calculate the tacticity after **sis** subsequences have been excluded from each of the three ranks (first and the two overlaps) we obtain the tacticity of the crystallizable sequences. A similar determination was made of the **siiis** units, while the exclusion of the longer subsequences has a negligible effect and is not considered. The crystal tacticities are plotted in *Figure 13*. The overall values for the crystals were found by calculating the α values after the exclusion of the **siiis** subsequences first, and then using these as the effective starting values for the subsequent calculation of α with **sis** sequences missing too.